

**$\Lambda$ -enhanced gray-molasses cooling of cesium atoms on the  $D_2$  line**Ya-Fen Hsiao,<sup>1,2</sup> Yu-Ju Lin,<sup>1</sup> and Ying-Cheng Chen<sup>1,\*</sup><sup>1</sup>*Institute of Atomic and Molecular Sciences, Academia Sinica, Taipei 10617, Taiwan*<sup>2</sup>*Molecular Science Technology, Taiwan International Graduate Program, Academia Sinica and National Central University, Taipei 10617, Taiwan*

(Received 19 July 2018; published 28 September 2018)

We present a systematic study of the  $\Lambda$ -enhanced gray molasses cooling ( $\Lambda$ -GMC) of cesium atoms on the  $D_2$  transition. Due to the large splitting in the excited hyperfine transitions of the cesium  $D_2$  line, it is relatively simple to implement the  $\Lambda$ -GMC with a suitable frequency control of the trapping and repumping lasers of the magneto-optical trap (MOT). We achieve a temperature of  $1.7 \pm 0.2 \mu\text{K}$  with  $3.2 \times 10^8$  atoms. The phase space density of atoms is  $1.43 \times 10^{-4}$ . Compared to the condition with a bare MOT or a MOT with gray-molasses cooling without  $\Lambda$  enhancement, there is an increase in the phase space density by a factor of more than  $10^3$  and  $10$ , respectively.

DOI: [10.1103/PhysRevA.98.033419](https://doi.org/10.1103/PhysRevA.98.033419)**I. INTRODUCTION**

Laser cooling and trapping of atoms in magneto-optical traps and optical molasses [1], developed around the 1980s, has become a starting point for many experiments on quantum optics and quantum many-body physics. The sub-Doppler cooling based on the polarization gradients and optical pumping among Zeeman sublevels in optical molasses with a red-detuned cooling laser driving the  $F \rightarrow F' = F + 1$  cycling transition leads to a temperature below the Doppler temperature limit [2–4]. Around the middle 1990s, a variant sub-Doppler cooling mechanism was proposed [5] and demonstrated [6–8] in which a blue-detuned cooling laser driving the  $F \rightarrow F' = F$  or  $F \rightarrow F' = F - 1$  open transition is used. Because atoms can be optically pumped to Zeeman dark states with a significantly reduced fluorescence rate once they are cold, this cooling method is also called gray-molasses cooling (GMC) while the cooling with a cycling transition is called bright-molasses cooling (BMC). The GMC allows one to achieve an even colder temperature and a higher atom density compared to the BMC. With either of the sub-Doppler cooling methods, it is advantageous to increase the phase space density of atoms when loading them to either magnetic traps or optical dipole traps for evaporative cooling to quantum degeneracy.

Sub-Doppler cooling is usually considered as likely be ineffective for the  $D_2$  transition of lithium and potassium, especially their bosonic isotopes, due to the narrow excited-state structure [9]. However, more careful studies have shown that one still can achieve a sub-Doppler temperature by sophisticated dynamic control of the intensity and detuning of the cooling and repumping lasers [10,11]. Recently, the success of blue-detuned,  $\Lambda$ -enhanced sub-Doppler cooling of  $^{40}\text{K}$  [12],  $^{39}\text{K}$  [13], and  $^7\text{Li}$  [14] has attracted renewed interest in laser cooling based on dark states. Under the Raman (two-photon)

resonance condition for the two lasers driving the  $F \rightarrow F' = F$  and  $F - 1 \rightarrow F' = F$  open transitions, atoms are optically pumped to the dark states formed by coherent superposition of the two ground-state hyperfine manifolds once they are cold. Due to the  $\Lambda$ -type laser excitation scheme and Raman coherences involved, this method is also called  $\Lambda$ -enhanced gray-molasses cooling ( $\Lambda$ -GMC).  $\Lambda$ -GMC has been demonstrated to occur in many other atomic species and isotopes, such as  $^6\text{Li}$  [15,16],  $^{23}\text{Na}$  [17,18],  $^{39}\text{K}$  [19],  $^{40}\text{K}$  [16,20],  $^{41}\text{K}$  [21], and  $^{87}\text{Rb}$  [22]. In most of the works examining Li, K, and Na, the  $\Lambda$ -GMC was implemented with the  $D_1$  transition or the  $D_2$  transition, which have well-separated hyperfine spacing. Thanks to the large hyperfine splitting in the  $D_2$  transition of  $^{87}\text{Rb}$  and  $^{133}\text{Cs}$ ,  $\Lambda$ -GMC can be easily implemented by using trapping and repumping lasers with suitable frequency control. Although there are other cooling schemes, such as degenerate Raman sideband cooling [23], that allow one to cool atoms to sub- $\mu\text{K}$  temperature, they require more lasers and a relatively complicated setup.  $\Lambda$ -GMC provides a simple and effective way to increase the phase space density of the atoms, which facilitates the loading into optical dipole traps for further cooling to quantum degeneracies [15,21]. In this paper, we report on the  $\Lambda$ -GMC of  $^{133}\text{Cs}$  to  $1.7 \pm 0.2 \mu\text{K}$  with a number of atom being  $3.2 \times 10^8$ . This brings a closure of the demonstration of  $\Lambda$ -GMC for stable alkali species. Table I gives a summary of the alkali species and isotopes that  $\Lambda$ -GMC have been implemented. Recently, this cooling method has also been applied to SrF and CaF molecules [24,25].

The theoretical aspects of  $\Lambda$ -GMC have been studied [14,19,22]. Using a one-dimensional model in a  $\Lambda$ -type three-level system, one can calculate the friction coefficient and the photon scattering rate based on the optical Bloch equation under certain approximations. A narrow dispersive feature in the friction coefficient around the Raman resonance condition appears with the red (blue)-detuned side of the two-photon detuning favoring the cooling (heating) force in the case of one-photon blue-detuned for both lasers. The photon scattering rate reaches a minimum at the exact

\*chenyc@pub.iam.s.sinica.edu.tw

TABLE I. A summary of alkali species and isotopes that  $\Lambda$ -enhanced gray-molasses cooling have been implemented. Which transition (either  $D_1$  or  $D_2$ ) that  $\Lambda$ -GMC was implemented and the minimum achieved temperatures are also shown.

Atomic Species	$^6\text{Li}$	$^7\text{Li}$	$^{23}\text{Na}$	$^{23}\text{Na}$	$^{39}\text{K}$	$^{40}\text{K}$	$^{40}\text{K}$	$^{41}\text{K}$	$^{87}\text{Rb}$	$^{133}\text{Cs}$
Min Temp ( $\mu\text{K}$ )	40/44	60	9	56	6/12	20/11	48	42	4	1.7
$D_1/D_2$ Line	$D_1$	$D_1$	$D_1$	$D_2$	$D_1$	$D_1$	$D_2$	$D_1$	$D_2$	$D_2$
Reference	[15]/[16]	[14]	[17]	[18]	[13]/[19]	[12]/[16]	[20]	[21]	[22]	This work

Raman resonance, rising sharply on the blue-detuned side but relatively slowly on the red-detuned side. The equilibrium temperature is determined by both the friction coefficient and the photon scattering rate. The degree of Raman coherence of the dark state directly affects the minimum photon scattering rate, and thus the temperature. As known in dark state physics, the mutual laser coherence, the magnetic field, and its inhomogeneity, etc. may affect the Raman coherence [26]. These parameters should be well controlled to reach a low temperature.

We detail our experimental setup in Sec. II and present the results and discussions in Sec. III, followed by a conclusion.

## II. EXPERIMENTAL SETUP

Our cesium magneto-optical trap (MOT) was implemented in a glass cell with six independent trapping and repumping beams. Typically, we have  $\sim 20$  and  $\sim 12$  mW per beam for the trapping and repumping light, respectively. The power of the trapping and repumping beams can be tuned by controlling the driving radio-frequency (rf) power of the acousto-optic modulator (AOM) through a voltage-controlled attenuator. The diameters of the trapping and repumping beams are  $\sim 23$  mm. Two cesium dispensers are placed close to the MOT region and operated at a current of  $\sim 3$  A. Typically, we trapped  $\sim 4 \times 10^8$  atoms in the MOT.

The relevant energy levels of cesium and laser excitations are shown in Fig. 1(a). A master laser was locked to the crossover of the  $|F = 4\rangle \rightarrow |F' = 4\rangle$  and  $|F = 4\rangle \rightarrow |F' = 5\rangle$  transitions of cesium  $D_2$  line. Part of its light passed through a fiber electro-optic modulator (EOM 1) with the +1 order sideband injection locking an intermediate laser (IL1). Part of the light of IL1 passed through an AOM in a double-pass configuration that then seeded a tapered amplifier. The output of the amplifier passed one AOM and was then coupled into a  $2 \times 6$  fiber beam splitter (OZ Optics NEW FUSED-26-850-5/125-16.7-3S-3-2-PM-SF) to act as the repumping light. The frequency of the repumping light was on the resonance of the  $|F = 3\rangle \rightarrow |F' = 4\rangle$  transition under normal MOT operation. During the  $\Lambda$ -GMC stage, the frequency of the repumping light jumped to the blue side of the  $|F = 3\rangle \rightarrow |F' = 4\rangle$  transition (with a detuning denoted as  $\Delta_{\text{rp}}$ ) and acted as the repumping laser for  $\Lambda$ -GMC by controlling the driving frequency of the double-passed AOM. We kept the driving frequency of the EOM 1 fixed, although a larger frequency tuning range was allowed. This was because part of the light from EOM 1 was also used for another MOT system in the laboratory and both systems were under operation simultaneously. Another part of the IL1 passed through another fiber-EOM (EOM 2) with its  $-1$  order sideband injection locking one intermediate laser (IL2). The

light of IL2 seeded another tapered amplifier. The output of this amplifier passed through one AOM and was then coupled into the  $2 \times 6$  fiber splitter to act as the trapping light. The frequency of the trapping light could be switched to the blue side of the  $|F = 4\rangle \rightarrow |F' = 4\rangle$ , whose detuning with respect to this transition is denoted as  $\Delta$ , by changing the driving frequency of the fiber EOM 2. It acted as the cooling light for the  $\Lambda$ -GMC. The two-photon detuning for the  $\Lambda$ -GMC repumping relative to the cooling light is denoted as  $\delta (= \Delta_{\text{rp}} - \Delta)$ , as shown in Fig. 1(a).

Three pairs of coils were used to compensate the stray magnetic fields. We used microwave spectroscopy to diagnose the magnitude of the magnetic field and calibrate the magnetic field per current for each pair of compensation coils. Based on these, it was relatively easy to nullify the stray magnetic field to a few mG levels, which is crucial to reach a low atomic temperature by  $\Lambda$ -GMC.

Our timing diagram is shown in Fig. 1(b). The experiment ran at a repetition rate of 7.5 Hz. At the end of the MOT loading period, the current for the MOT quadrupole magnetic field was turned off within 200  $\mu\text{s}$ . One ms later, the frequency of the trapping laser jumped to the detuning level for  $\Lambda$ -GMC, which was typically  $\Delta \approx 4.73\Gamma$ , unless specified, with its intensity remaining the same. The intensity and frequency of the repumping laser remained the same. For a duration of 2 ms, we took advantage of the gray-molasses cooling without  $\Lambda$  enhancement [6–8] to precool the atoms to  $\sim 8 \mu\text{K}$  before performing  $\Lambda$ -GMC. We also checked the performance of  $\Lambda$ -GMC directly from the MOT without GMC, in which the atomic temperature was around 120  $\mu\text{K}$ . We found no obvious gain, both in atom number and temperature, in using this precooling stage. We believe that is because the temperature in a cesium MOT is already relatively cold even without any precooling, compared to the case of lithium or potassium, which is in mK scale. In the case for lithium [15], the precooling does help the fraction of atom number captured after  $\Lambda$ -GMC but not the final temperature. However, we still chose timing with the 2-ms precooling for all data taking. Next, the repumping frequency was switched to the desired value for  $\Lambda$ -GMC, remaining constant for the following 4 ms. The intensities of both the trapping and repumping beams were also reduced to varying values to study their dependence on the performance of the  $\Lambda$ -GMC. The trapping and repumping light played the role of cooling and repumping light during the  $\Lambda$ -GMC stage. We denote the one-beam intensities of the  $\Lambda$ -GMC cooling and repumping light as  $I_{\text{cool}}$  and  $I_{\text{rep}}$ , respectively. In the subsequent 1 ms, the repumping light was turned off, and the population was optically pumped by the cooling light to the  $F = 3$  hyperfine ground state, which is the state desired for future experiments related to electromagnetically induced transparency. We then turned off all the lasers for a certain

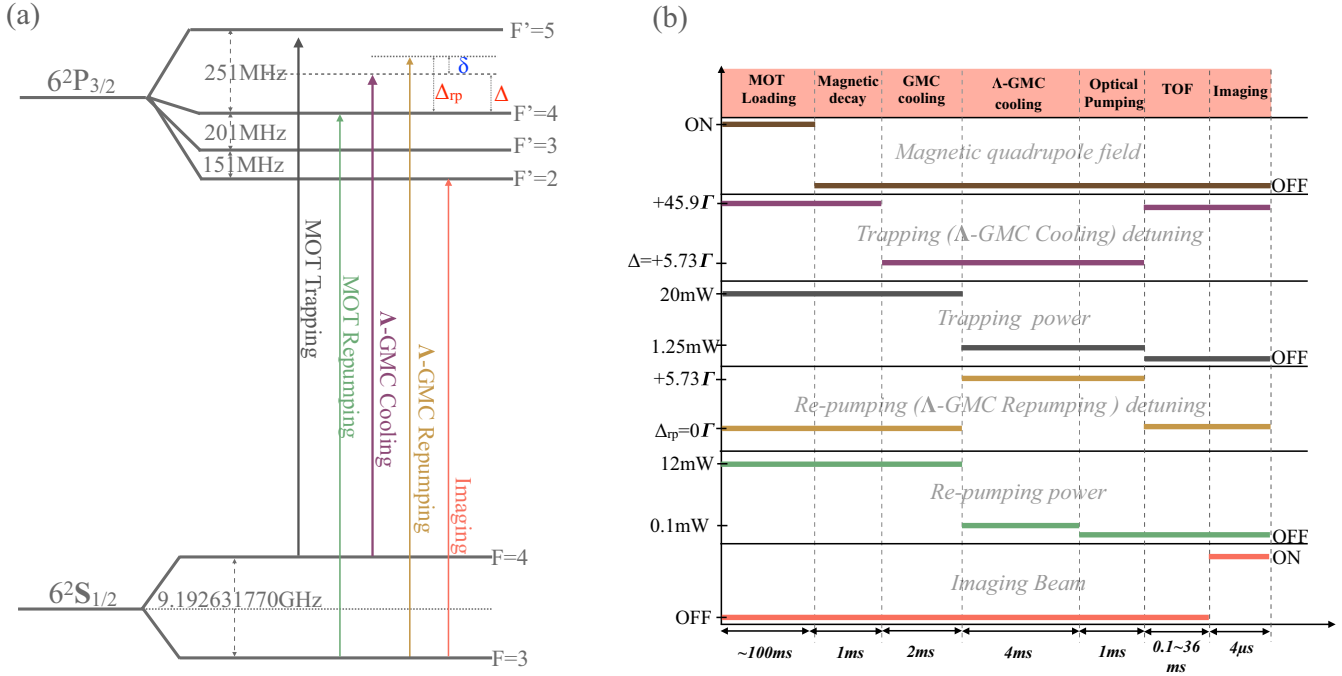


FIG. 1. (a) Energy levels of  $^{133}\text{Cs}$  and relevant laser excitations. The MOT trapping (repumping) beams also act as the  $\Lambda$ -GMC cooling (repumping) beams in the experiment.  $\Delta$  ( $\Delta_{\text{rp}}$ ) is the detuning of the  $\Lambda$ -GMC cooling (repumping) light with respect to  $|F = 4\rangle \rightarrow |F' = 4\rangle$  ( $|F = 3\rangle \rightarrow |F' = 4\rangle$ ) transition.  $\delta = \Delta_{\text{rp}} - \Delta$  is the two-photon detuning. (b) The timing diagram of the experiment.

flight time and fired the imaging beam, which drives the  $|F = 3\rangle \rightarrow |F' = 2\rangle$  transition.

From the absorption imaging, we determined the two-dimensional profile (referred to the  $x$  and  $z$  - axis, where  $z$  is the direction of gravity) of the column density. To allow quicker and more reliable fitting, we summed the column density along the  $x$  and  $z$  axis, respectively. The results were fitted to a one-dimensional Gaussian function to get the  $e^{-1}$  width in each axis ( $\sigma_i$ ,  $i = x, z$ ). Based on the fit width and amplitude, we obtained the atom number using an absorption cross section of  $\frac{5}{21} \frac{3\lambda^2}{2\pi}$  assuming a uniform population in the Zeeman sublevels and with a linearly polarized image beam, where  $\lambda = 852.35$  nm is the wavelength of the  $D_2$  transition. The atom temperature could be determined by fitting the  $e^{-1}$  width of the atomic clouds versus different flight times with the formula,

$$\sigma_i(t_{\text{TOF}}) = \sqrt{\sigma_{i,0}^2 + \frac{2k_B T_i}{m} t_{\text{TOF}}^2}. \quad (1)$$

The maximum flight time can be up to 36 ms for a temperature of  $\sim 2 \mu\text{K}$ . The position shift of the atomic clouds due to gravitational free-fall motion was used to determine the magnification ratio of the imaging system, allowing an accurate determination of the temperature. Our atomic clouds were elliptical with a width  $\sigma_x$  2–3 times larger than  $\sigma_z$ . The fitting result of  $T_x$  was not as reliable as that of  $T_z$ , since even longer flight times were needed to allow sufficient expansion in the cloud size. However, the images at longer flight times were limited by the size of the CCD chip. The atom temperatures shown in all figures are  $T_z$ .

### III. RESULTS AND DISCUSSIONS

We first studied the atom number and temperature dependence versus the  $\Lambda$ -GMC time at a zero two-photon detuning ( $\delta = 0$ ) and a one-photon detuning  $\Delta$  of  $5.73\Gamma$ , as shown in Fig. 2. During  $\Lambda$ -GMC, the one-beam cooling and repumping intensities ( $I_{\text{cool}}$  and  $I_{\text{rep}}$ ) were 0.273 and 0.022  $I_{\text{sat}}$ , respectively, where  $I_{\text{sat}} = 1.10$  mW/cm $^2$  is the saturation intensity of the cesium  $D_2$  transition. Prior to the  $\Lambda$ -GMC, the atoms had been cooled to  $8.4 \mu\text{K}$  by gray molasses cooling without  $\Lambda$ -enhancement for 2 ms. With a  $\Lambda$ -GMC time of  $> \sim 2$  ms, both the temperature and atom number reached a steady-state

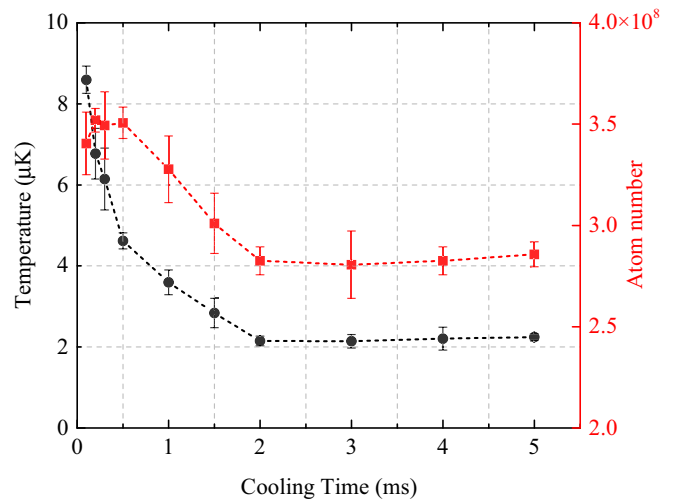


FIG. 2. Atom number (square) and temperature (circle) versus the  $\Lambda$ -enhanced gray-molasses cooling time.  $\delta = 0$  and  $\Delta = 5.73\Gamma$ .  $I_{\text{cool}} = 0.273 I_{\text{sat}}$ . and  $I_{\text{rep}}/I_{\text{cool}} = 0.08$ .

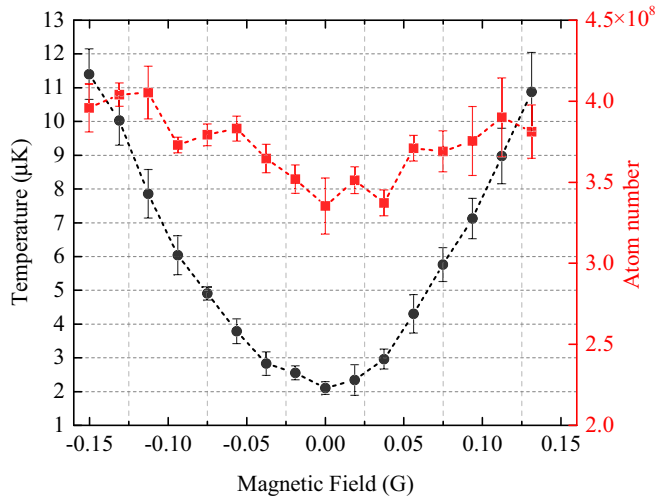


FIG. 3. Atom number (square) and temperature (circle) after 4-ms  $\Lambda$ -GMC versus the magnetic field.  $\delta = 0$  and  $\Delta = 5.73\Gamma$ .  $I_{\text{cool}} = 0.273I_{\text{sat}}$ , and  $I_{\text{rep}}/I_{\text{cool}} = 0.08$ .

value. We observed a  $\sim 20\%$  reduction in the atom number and a fourfold reduction in temperature at the steady state. Because we decreased the laser power suddenly to a lower value, the cooling force also decreased significantly and was not sufficient to capture atoms with larger velocities. This caused some atom losses during the molasses stage. This atom loss could be avoided if one gradually decreased the laser power [17], although we did not implement this in this work. In all later studies, we chose a  $\Lambda$ -GMC duration of 4 ms.

#### A. Magnetic field dependence

Because  $\Lambda$ -GMC utilizes the dark state, it is expected that the ground-state decoherence rate plays an important role in the cooling performance. During the cooling period, atoms may be distributed among different Zeeman sublevels. Minimization of the stray magnetic field effectively reduces the distribution in the Zeeman shifts and thus the ground-state decoherence rate. A smaller decoherence rate for the dark state results in a smaller fluorescence (heating) rate and thus a lower temperature. Figure 3 depicts the atom number and temperature versus the magnetic field, obtained by controlling the current through one pair of the compensation coils. The temperature shows a quadratic dependence on the magnetic field [12] as  $\Delta T = 532B^2 \mu K / G^2$ . The stray magnetic field needed to be canceled to less than 14 mG to have a negligible increase ( $<5\%$ ) in the temperature.

Another critical factor that affects the decoherence rate of the dark state is the mutual coherence between the cooling and repumping lasers. It has been found that the laser mutual coherence significantly affects the minimum temperature [22]. The minimum temperature achieved with the cooling and repumping lasers being injection locked to the same master laser is much lower than that achieved with the two lasers independently locked [22]. Since our cooling and repumping lasers were injection locked to the same master laser with frequency offsets determined by the EOMs or AOMs driven by stable signal generators (stabilities  $<10^{-10}$ ), the laser mutual coherence should not be the major limitation in the minimum temperature.

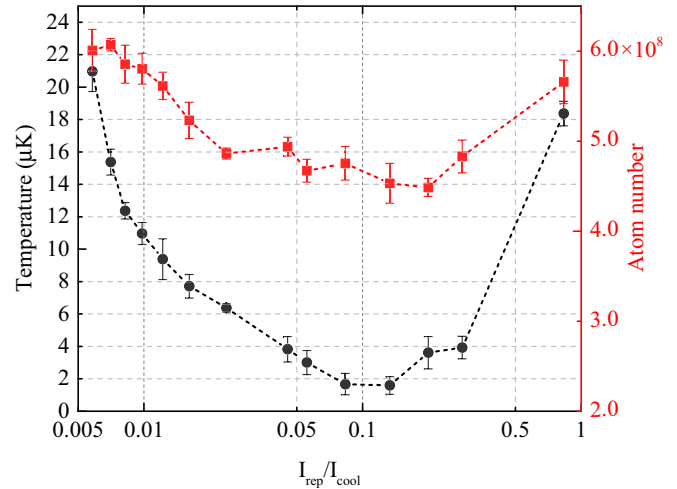


FIG. 4. Atom number (square) and temperature (circle) after 4-ms  $\Lambda$ -GMC versus the intensity ratio of repumping to cooling beam.  $\delta = 0$  and  $\Delta = 5.73\Gamma$ .  $I_{\text{rep}} = 0.022I_{\text{sat}}$ .

#### B. Intensity dependence

At a  $\Delta$  of  $5.73\Gamma$  and a zero  $\delta$ , we varied the intensity of the  $\Lambda$ -GMC cooling beam ( $I_{\text{cool}}$ ) while keeping the repumping beam intensity ( $I_{\text{rep}}$ ) fixed at  $0.023I_{\text{sat}}$  and measured the atom number and temperature dependence on the intensity ratio ( $I_{\text{rep}}/I_{\text{cool}}$ ). The results are shown in Fig. 4. We found an optimal intensity ratio of around 0.08 where the temperature reached a minimum. When decreasing  $I_{\text{cool}}$  so that the intensity ratio was much larger than 0.08, the temperature rose. This might be due to the ceased working of  $\Lambda$ -GMC when both laser intensities were too weak. We also checked the same dependence at different  $I_{\text{rep}}$ , and found that the minimum temperature occurred at roughly the same intensity ratio.

We then kept the intensity ratio fixed at 0.08 and varied the power of both beams during the  $\Lambda$ -GMC period. The atom

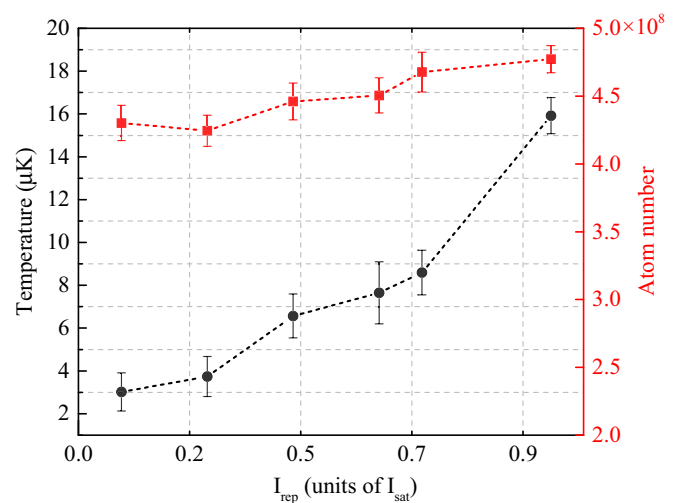


FIG. 5. Atom number (square) and temperature (circle) after 4-ms  $\Lambda$ -GMC versus the intensity of repumping beam.  $I_{\text{rep}}/I_{\text{cool}} = 0.08$ .  $\delta = 0$ , and  $\Delta = 5.73\Gamma$ .



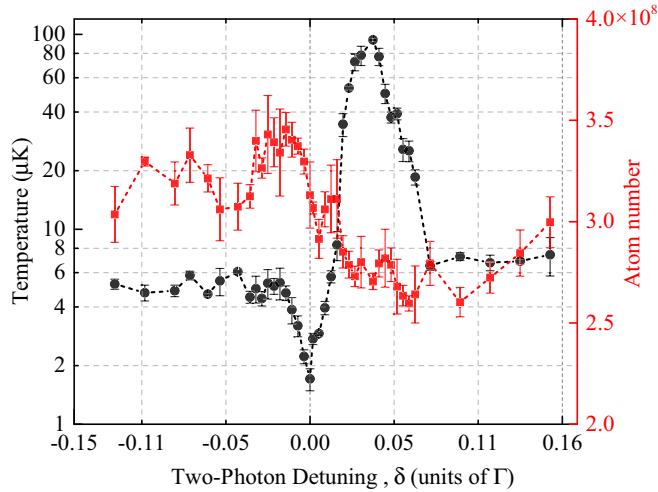


FIG. 6. Atom number (square) and temperature (circle) after 4-ms  $\Lambda$ -GMC versus the two-photon detuning  $\delta$ .  $\Delta = 5.73 \Gamma$ .  $I_{\text{cool}} = 0.273 I_{\text{sat}}$ , and  $I_{\text{rep}}/I_{\text{cool}} = 0.08$ .

number and temperature versus the repumping beam intensity is shown in Fig. 5. The results show that the temperature monotonically increases with the laser intensity. There is a slight reduction in the atom number for lower laser intensities. This is expected since atoms with larger velocities may leave the trap due to weaker trapping forces.

### C. Detuning dependence

#### 1. Two-photon detuning

At a  $\Delta$  of  $5.73\Gamma$  and an intensity ratio of 0.08, we varied the detuning of the  $\Lambda$ -GMC repumping beams and measured the atom number and temperature versus the two-photon detuning  $\delta$ , as shown in Fig. 6. The lowest temperature of  $1.7 \pm 0.2 \mu\text{K}$  appeared at  $\delta = 0$ , which is a characteristic for  $\Lambda$ -GMC. At  $\delta = 0$ , the captured atom number was  $\sim 80\%$  of that before  $\Lambda$ -GMC, which is  $3.7 \times 10^8$ . For blue detunings ( $\delta > 0$ ), the temperature rose sharply up to  $\sim 100 \mu\text{K}$  while the atom number dropped slightly. The phase space density at the lowest temperature was  $1.43 \times 10^{-4}$ . Compared to the condition before  $\Lambda$ -GMC, it increased by more than a factor of 10. Compared to the bare MOT without precooling, which had a temperature of  $120 \mu\text{K}$ , the phase space density rose by more than a factor of 1000.

#### 2. One-photon detuning

We then kept the two-photon detuning fixed at zero and measured the atom number and temperature dependence on

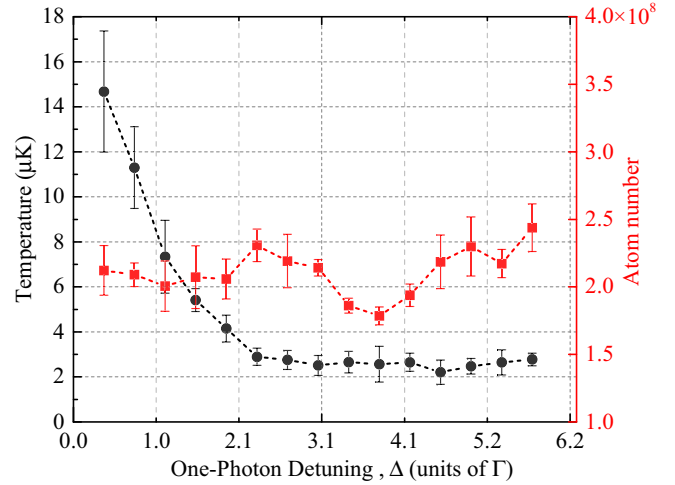


FIG. 7. Atom number (square) and temperature (circle) after 4-ms  $\Lambda$ -GMC versus the one-photon detuning  $\Delta$ .  $\delta = 0$ .  $I_{\text{cool}} = 0.273 I_{\text{sat}}$ , and  $I_{\text{rep}}/I_{\text{cool}} = 0.08$ .

the one-photon detuning  $\Delta$ , as shown in Fig. 7. The temperatures decreased and reached an almost constant value as  $\Delta$  increased. Limited by the frequency tuning range of the double-passed AOM, the maximum  $\Delta$  was  $5.73 \Gamma$ . Similar behaviors have been observed in many other works [18,20,22]. As  $\Delta$  increases further, we expect that the temperature would rise at some point, since the cooling laser may drive the  $|F = 4\rangle \rightarrow |F' = 5\rangle$  cycling transition significantly and degrade the Raman coherence of the dark states due to the spontaneous decay [18].

### IV. CONCLUSION

In conclusion, we performed a systematic study of  $\Lambda$ -enhanced gray-molasses cooling of cesium with the  $D_2$  line. The lowest temperature of  $1.7 \pm 0.2 \mu\text{K}$  was achieved. The  $\Lambda$ -GMC provided a simple and effective way to increase the phase space density for further magnetic or optical dipole trap loading and evaporative cooling towards quantum degeneracy.

### ACKNOWLEDGMENTS

We thank Ming-Shien Chang for input and useful discussions. We acknowledge the financial support from the Ministry of Science and Technology, Taiwan under Grants No. 103-2112-M-001-010-MY3 and No. 106-2119-M-001-002. We also thank the support from the Physics Division, National Center for Theoretical Sciences, Taiwan and Center for Quantum Technology, Taiwan.

[1] E. L. Raab, M. Prentiss, A. Cable, S. Chu, and D. E. Pritchard, *Phys. Rev. Lett.* **59**, 2631 (1987).  
 [2] J. Dalibard and C. Cohen-Tannoudj, *J. Opt. Soc. Am. B* **11**, 2023 (1989).  
 [3] D. S. Weiss, E. Riis, Y. Shevy, P. J. Ungar, and S. Chu, *J. Opt. Soc. Am. B* **11**, 2072 (1989).

[4] P. D. Lett, W. D. Phillips, S. L. Rolston, C. E. Tanner, R. N. Watts, and C. I. Westbrook, *J. Opt. Soc. Am. B* **11**, 2084 (1989).  
 [5] G. Grynberg and J.-Y. Courtois, *Europhys. Lett.* **27**, 41 (1994).  
 [6] D. Boiron, A. Michaud, P. Lemonde, Y. Castin, C. Salomon, S. Weyers, K. Szymaniec, L. Cognet, and A. Clairon, *Phys. Rev. A* **53**, R3734 (1996).

- [7] T. Esslinger, F. Sander, A. Hemmerich, T. W. Hänsch, H. Ritsch, and M. Weidemüller, *Opt. Lett.* **13**, 991 (1996).
- [8] C. Triché, P. Verkerk, and G. Grynberg, *Eur. Phys. J. D* **5**, 225 (1999).
- [9] A. Bambini and A. Agresti, *Phys. Rev. A* **56**, 3040 (1997).
- [10] M. Landini, S. Roy, L. Carcagní, D. Trypogeorgos, M. Fattori, M. Inguscio, and G. Modugno, *Phys. Rev. A* **84**, 043432 (2011).
- [11] V. Gokhroo, G. Rajalakshmi, R. K. Easwaran, and C. S. Unnikrishnan, *J. Phys. B* **44**, 115307 (2011).
- [12] D. Rio Fernandes, F. Sievers, N. Kretzschmar, S. Wu, C. Salomon, and F. Chevy, *Europhys. Lett.* **100**, 63001 (2012).
- [13] G. Salomon, L. Fouch, P. Wang, A. Aspect, P. Bouyer, and T. Bourdel, *Europhys. Lett.* **104**, 63002 (2013).
- [14] A. T. Grier, I. Ferrier-Barbut, B. S. Rem, M. Delehaye, L. Khaykovich, F. Chevy, and C. Salomon, *Phys. Rev. A* **87**, 063411 (2013).
- [15] A. Burchianti, G. Valtolina, J. A. Seman, E. Pace, M. De Pas, M. Inguscio, M. Zaccanti, and G. Roati, *Phys. Rev. A* **90**, 043408 (2014).
- [16] F. Sievers, N. Kretzschmar, D. R. Fernandes, D. Suchet, M. Rabinovic, S. Wu, C. V. Parker, L. Khaykovich, C. Salomon, and F. Chevy, *Phys. Rev. A* **91**, 023426 (2015).
- [17] G. Colzi, G. Durastante, E. Fava, S. Serafini, G. Lamporesi, and G. Ferrari, *Phys. Rev. A* **93**, 023421 (2016).
- [18] Z. Shi, P. Wang, Z. Li, Z. Meng, L. Huang, and J. Zhang, [arXiv:1803.05108](https://arxiv.org/abs/1803.05108).
- [19] D. Nath, R. K. Easwaran, G. Rajalakshmi, and C. S. Unnikrishnan, *Phys. Rev. A* **88**, 053407 (2013).
- [20] G. D. Bruce, E. Haller, B. Peaudecerf, D. A. Cotta, M. Andia, S. Wu, M. Y. H. Johnson, B. W. Lovett, and S. Kuhr, *J. Phys. B* **50**, 095002 (2017).
- [21] H.-Z. Chen, X.-C. Yao, Y.-P. Wu, X.-P. Liu, X.-Q. Wang, Y.-X. Wang, Y.-A. Chen, and J.-W. Pan, *Phys. Rev. A* **94**, 033408 (2016).
- [22] S. Rosi, A. Burchianti, S. Conclave, D.-S. Naik, G. Roati, C. Fort, and F. Minardi, *Sci. Rep.* **8**, 7 (2018).
- [23] V. Vuletić, C. Chin, A. J. Kerman, and S. Chu, *Phys. Rev. Lett.* **81**, 5768 (1998).
- [24] D. J. McCarron, M. H. Steinecker, Y. Zhu, and D. DeMille, *Phys. Rev. Lett.* **121**, 013202 (2018).
- [25] L. W. Cheuk, L. Anderegg, B. L. Augenbraun, Y. Bao, S. Burchesky, W. Ketterle, and J. M. Doyle, *Phys. Rev. Lett.* **121**, 083201 (2018).
- [26] Y.-F. Hsiao, P.-J. Tsai, H.-S. Chen, S.-X. Lin, C.-C. Hung, C.-H. Lee, Y.-H. Chen, Y.-F. Chen, I. A. Yu, and Y.-C. Chen, *Phys. Rev. Lett.* **120**, 183602 (2018).